THE OFFICIAL MAGAZINE OF THE OCEANOGRAPHY SOCIETY

Oceanography

CITATION

Palevsky, H.I., and D.P. Nicholson. 2018. The North Atlantic biological pump: Insights from the Ocean Observatories Initiative Irminger Sea Array. *Oceanography* 31(1):42–49, https://doi.org/10.5670/oceanog.2018.108.

DOI

https://doi.org/10.5670/oceanog.2018.108

The North Atlantic Biological Pump

INSIGHTS FROM THE OCEAN OBSERVATORIES INITIATIVE IRMINGER SEA ARRAY

By Hilary I. Palevsky and David P. Nicholson

ABSTRACT. The biological pump plays a key role in the global carbon cycle by transporting photosynthetically fixed organic carbon into the deep ocean, where it can be sequestered from the atmosphere over annual or longer time scales if exported below the winter ventilation depth. In the subpolar North Atlantic, carbon sequestration via the biological pump is influenced by two competing forces: a spring diatom bloom that features large, fast-sinking biogenic particles, and deep winter mixing that requires particles to sink much further than in other ocean regions to escape winter ventilation. We synthesize biogeochemical sensor data from the first two years of operations at the Ocean Observatories Initiative Irminger Sea Array of moorings and gliders (September 2014–July 2016), providing the first simultaneous year-round observations of biological carbon cycling processes in both the surface ocean and the seasonal thermocline in this critical but previously undersampled region. These data show significant mixed layer net autotrophy during the spring bloom and significant respiration in the seasonal thermocline during the stratified season (~5.9 mol C m^{-2} remineralized between 200 m and 1,000 m). This respired carbon is subsequently ventilated during winter convective mixing (>1,000 m), a significant reduction in potential carbon sequestration. This highlights the importance of year-round observations to accurately constrain the biological pump in the subpolar North Atlantic, as well as other high-latitude regions that experience deep winter mixing.

Photo credit: Sheri White, © Woods Hole Oceanographic Institution

INTRODUCTION

Export of biologically fixed organic carbon from the surface to the deep ocean, known as the biological pump, plays an important role in the global carbon cycle (Volk and Hoffert, 1985). Photosynthesis by marine phytoplankton fixes carbon dioxide into organic carbon at a global rate of ~50 Pg yr^{-1} (Field et al., 1998). A fraction of this fixed organic carbon escapes being respired by organisms in the surface ocean and is transferred as sinking particles, by mixing of dissolved and suspended organic matter, and by vertical animal migration to the ocean interior, where it is sequestered from the atmosphere on time scales of months to centuries (Volk and Hoffert, 1985; DeVries et al., 2012). This process of biological carbon export is commonly known as the biological pump because it transfers carbon against a concentration gradient from the surface to the deep ocean, which maintains an inorganic carbon reservoir ~45 times that of the atmosphere (Volk and Hoffert, 1985; Sarmiento and Gruber, 2006; Ciais et al., 2013).

Current understanding suggests that anthropogenic carbon uptake to date has been predominantly driven by the abiotic solubility pump as the surface ocean equilibrates with rising atmospheric CO_2 concentrations, rather than by biological carbon cycling (Sabine and Tanhua, 2010). However, estimates of the current global rate of carbon transfer from the surface ocean to the interior via the biological pump, amounting to ~6–13 Pg C yr^{-1} (Laws et al., 2011; Siegel et al., 2014), significantly exceed the current rate at which the ocean absorbs atmospheric CO_2, estimated at 2.6 ± 0.5 Pg C yr^{-1} (Le Quéré et al., 2016), indicating that even a small perturbation to the biological pump could have a large influence on the global carbon cycle. Changes to the strength of the biological pump would also influence the distribution of nutrients and oxygen in the ocean, with broad implications for ocean ecosystems.

In order to effectively monitor and predict future changes to the ocean's biological pump, accurate baseline measurements of current rates of biological carbon export are necessary to validate rates predicted by remote-sensing algorithms and global climate models (e.g., Stukel et al., 2015; Palevsky et al., 2016b), as well as to refine our understanding of the processes controlling the biological pump. Our current understanding is limited, however, by the difficulty of measuring biological carbon export and the processes that drive it over the entire annual cycle. Our most detailed understanding of the biological pump and its role in the ocean carbon sink comes from time-series sites with robust sampling programs for both primary and export production, often with additional observations of ecosystem composition and structure useful for determining mechanistic controls on export (e.g., Church et al., 2013). However, these existing time-series sites are representative of only a small fraction of the global ocean (estimated at 9%–15% of the total ocean area; Henson et al., 2016), and year-round study sites are largely limited to the subtropical and tropical ocean, while high-latitude sites are sampled predominantly during the spring and summer productive season.

Year-round sampling of the biological pump is especially critical in high-latitude regions because a large fraction of the carbon exported seasonally during the spring and summer can be brought back to the surface and ventilated during deep winter mixing. For the biological pump to effectively sequester carbon from the atmosphere on annual or multi-annual timescales, organic material must sink deep enough to escape being entrained back into the deepest winter mixed layers. If sinking organic carbon is remineralized (converted from organic to inorganic carbon by respiration) within the seasonal thermocline (the portion of the water column below the seasonally stratified mixed layer but above the depth of deepest annual mixing), this carbon can ventilate back to the atmosphere as CO_2 when entrained into the wintertime mixed layer (Figure 1). Observational estimates based on year-round surface measurements in deep mixing regions in the western North Pacific, northeastern Atlantic, and subpolar North Atlantic indicate that 40%–90% of the organic carbon exported from the seasonally stratified mixed layer is subsequently ventilated during winter mixing (Körtzinger et al., 2008; Quay et al., 2012; Palevsky et al., 2016a). The rate of carbon sequestration below the winter ventilation depth depends not only on export from the euphotic zone during the productive season but also on respiration rates within the seasonal thermocline and the depth of physical mixing the subsequent winter.

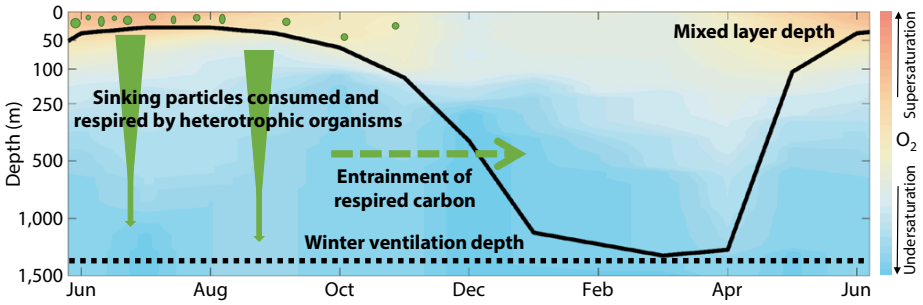

FIGURE 1. Schematic seasonal cycle of organic carbon export and winter ventilation in the subpolar North Atlantic (oxygen saturation and mixed layer depth based on World Ocean Atlas 2013 data for the OOI Irminger Sea Array site). Phytoplankton growth in the spring and summer leads to export from the seasonally stratified mixed layer. This surface net autotrophy is evident in mixed layer oxygen supersaturation. However, much of the seasonally exported carbon is remineralized in the seasonal thermocline and entrained back into the mixed layer during deep winter mixing. This ventilates the respired carbon (and waters undersaturated with oxygen due to net respiration) back to the atmosphere. In order for carbon to be sequestered on annual or longer time scales, it must sink below the winter ventilation depth prior to remineralization.

In this paper, we focus on the Irminger Sea region of the subpolar North Atlantic as a case study of the high-latitude biological pump. The subpolar North Atlantic is a strong carbon sink region where the biological carbon pump's annual cycle features two pronounced and competing processes: a spring diatom bloom that produces large, fast-sinking particles, and deep winter mixing that ventilates carbon remineralized in the seasonal thermocline back to the atmosphere (Figures 1 and 2a). The Ocean Observatories Initiative (OOI) Irminger Sea Array of moorings and gliders provides a unique opportunity to study the subpolar North Atlantic biological carbon pump throughout the year within the context of an unprecedented density of biogeochemical, physical, and bio-optical sensors operating for multiple years at high temporal resolution. We synthesize data from the OOI Irminger Sea Array's first two years of operation, illustrating the full annual cycle of biologically driven carbon cycling processes in both the surface ocean and the seasonal thermocline in this globally significant and previously undersampled high-latitude region.

THE SUBPOLAR NORTH ATLANTIC AND THE IRMINGER SEA

Anthropogenic carbon has accumulated in the North Atlantic at approximately three times the global average rate (Sabine et al., 2004; Khatiwala et al., 2009), making it a region of critical importance for understanding the ocean's role in carbon cycling. Deepwater formation in the subpolar North Atlantic enhances the ability of the ocean to absorb carbon abiotically via the solubility pump (Sabine and Tanhua, 2010), and also increases the sequestration time for biologically exported carbon that reaches below the winter ventilation depth (DeVries et al., 2012). However, the amount of carbon sequestered annually by the biological pump and its role in driving ocean carbon uptake in the subpolar North Atlantic is not well constrained (Sanders et al., 2014).

A dominant feature of the subpolar North Atlantic seasonal cycle is the large, diatom-dominated spring phytoplankton bloom (Figure 2a; for a review of the bloom and its drivers, see Behrenfeld and Boss, 2014). Many prior studies have documented high rates of primary production and organic carbon export from the surface ocean during the bloom (e.g., Buesseler et al., 1992; Quay et al., 2012). Fast-sinking particles and aggregates can transfer this organic carbon to depth, with significant particle fluxes observed between the base of the euphotic zone and 1,000 m (Antia et al., 2001; Briggs et al., 2011; P. Martin et al., 2011). Dissolved and suspended organic matter can also be transferred from the surface mixed layer to the thermocline by episodic mixing followed by restratification (Dall'Olmo et al., 2016). However, this organic matter must penetrate below the deepest winter mixing depth in order not to be remineralized in the seasonal thermocline and ventilated back to the atmosphere during the subsequent winter (Figure 1; Oschlies and Kahler, 2004; Körtzinger et al., 2008; Quay et al., 2012).

The Irminger Sea, located between Greenland and Iceland (Figure 2a), experiences both the large spring bloom and deep winter mixing characteristic throughout the North Atlantic subpolar gyre. Strong wintertime atmospheric forcing over the Irminger Sea cools the surface ocean and drives winter convective mixing to depths of up to 1,400 m, forming a water mass that extends throughout the mid-depth North Atlantic (Pickart et al., 2003; de Jong et al., 2012; de Jong and de Steur, 2016; de Jong et al., 2018, in this issue). There is significant interannual variability in Irminger Sea convective mixing, with the deepest mixing occurring during years with the strongest surface cooling (associated with the positive phase of the North Atlantic Oscillation; de Jong and de Steur, 2016). There is also significant interannual variability in the magnitude and timing of the spring bloom, with satellite ocean color observations showing a delayed bloom and lower maximum chlorophyll *a* concentrations in positive phase North Atlantic Oscillation years

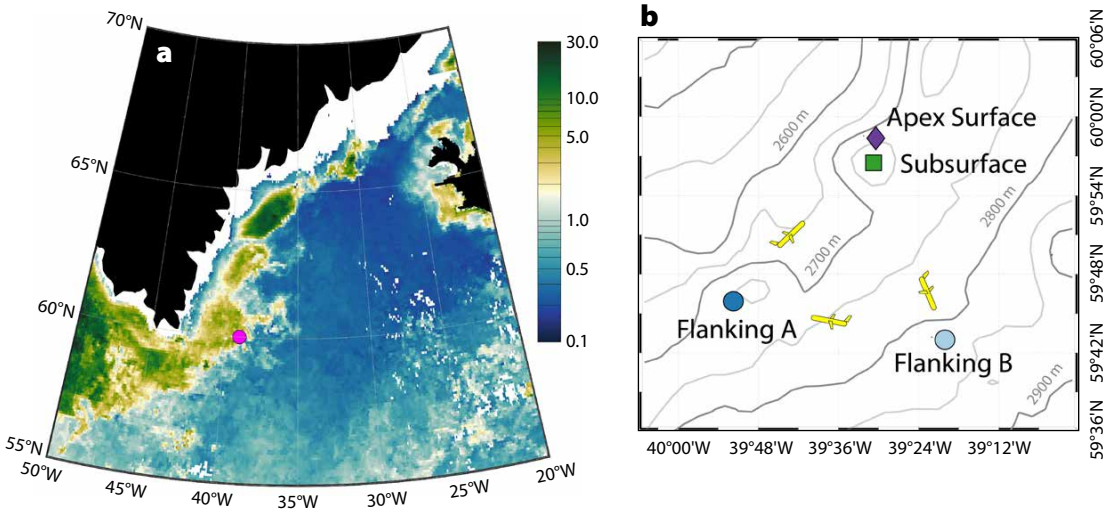

FIGURE 2. (a) Sea surface chlorophyll *a* (µg L^{-1}; 9 km MODIS Aqua) in the Irminger Sea from May 2015. The pink dot indicates the location of the OOI Irminger Sea Array. (b) Configuration of moorings and gliders at the OOI Irminger Sea Array, overlain on bathymetric contours.

that have stronger cooling and deeper mixing (Henson et al., 2006, 2009). This interannual variability in bloom dynamics and physical forcing likely also influences the amount of carbon seasonally exported from the surface ocean, remineralization rates in the seasonal thermocline, and the fraction of seasonally exported carbon ventilated during winter mixing. However, these connections cannot yet be disentangled, because long-term observations have historically been limited to physical properties and satellite ocean color, without corresponding tracers of the biological pump. The picture of the Irminger Sea biological pump presented here, based on the first two years of data from the OOI Array, provides an initial snapshot of the system within the context of longer-term interannual variability, which this new time series will enable us to resolve through continued collection of biogeochemical data over the coming years.

OOI IRMINGER SEA ARRAY

The OOI Irminger Sea Array was first deployed in September 2014, beginning an ongoing time series of observations planned to continue for 25 to 30 years. The array is arranged in a triangular configuration (nominally 20 km a side), with an Apex surface mooring co-located with a subsurface profiler mooring at the north point of the triangle and two flanking moorings located at the southern corners (Figure 2b). Up to three open-ocean gliders continually transit around the array triangle, diving from the surface to 1,000 m. Annual summertime cruises recover all moorings and gliders from the previous year and deploy replacements, as well as conduct shipboard calibration casts for sensors on all moorings and gliders.

Here, we synthesize data collected over the first two years of OOI Irminger Sea Array deployment (September 2014–July 2016) to trace organic carbon production, remineralization, and ventilation. We focus in particular on dissolved oxygen, as stable response Aanderaa optode model 4831 oxygen sensors are located on all moorings and gliders within the OOI Array, and provide a continuous picture of biologically mediated surface and subsurface carbon cycling. To provide physical and biological context, we interpret these oxygen data alongside temperature and salinity data collected on all moorings and gliders, and chlorophyll *a* concentrations determined from surface mooring fluorometers (see online Supplementary Text for full details on all data included in this analysis).

DISSOLVED OXYGEN DATA FROM THE OOI ARRAY

Dissolved oxygen is a commonly used tracer of the biological pump because it records the balance between rates of photosynthesis and respiration. In a net autotrophic system, photosynthesis dominates over respiration, leading to net biological production of dissolved oxygen that is stoichiometrically related to net production of organic carbon. Conversely, in a net heterotrophic system, oxygen losses due to respiration dominate and are stoichiometrically related to net consumption of organic carbon by remineralization. Abiotic processes of air-sea gas exchange and physical mixing also influence dissolved oxygen concentrations in the ocean, so interpretation of dissolved oxygen data to examine the effects of biological processes requires us to disentangle these separate influences.

Quantitative interpretation of dissolved oxygen sensor data requires that sensors be calibrated to account for two primary sources of error: (1) rapid drift from factory calibrations prior to deployment, and (2) in situ drift after deployment (D'Asaro and McNeil, 2013; Takeshita et al., 2013; Bittig and Körtzinger, 2015, 2017; Johnson et al., 2015; Bushinsky et al., 2016). Details of these corrections are provided in the Supplementary Text. We correct for pre-deployment drift using discrete samples for dissolved oxygen collected during the deployment cruises and measured using shipboard Winkler titrations, which remain the gold standard for accurate dissolved oxygen measurements. This enables us to determine sensor-specific gain corrections (Figure S1, Table S1). We correct for in situ drift by assuming that oxygen concentrations on deep isotherms (2,000 m and below) should be stable over time, and that observed oxygen change at these depths represents sensor drift (Figure S2, Table S2).

The surface mixed layer oxygen measurements are subject to greater uncertainty than the thermocline measurements due to greater uncertainty in their pre-deployment drift gain corrections and the faster drift of optodes measuring surface properties (Tables S1 and S2). We therefore do not use surface oxygen measurements to calculate air-sea oxygen flux or net community production, which require highly accurate surface oxygen measurements (Emerson and Bushinsky, 2014). Further study with more accurately constrained surface dissolved oxygen measurements will be needed to determine the relative roles of air-sea oxygen flux, biological production, and physical influences on mixed layer dissolved oxygen. Here, we qualitatively interpret the mixed layer seasonal cycle and focus quantitative interpretation on the spring bloom signal that is large enough to overwhelm uncertainty and on the more accurately constrained measurements of the seasonal thermocline from the profiler mooring.

SEASONAL CYCLE IN THE SURFACE OCEAN

The Irminger Sea surface mixed layer ranges from <30 m during the stratified summer season to depths of >1,000 m during winter, and shows a pronounced seasonal cycle in physical, biological, and chemical properties (Figure 3). Sea surface temperatures range from late winter minima of 3.5°–3.6°C to summer maxima of 9.5°C (Figure 3a). Previous analysis shows that the winter of 2014–2015 in the Irminger Sea was characterized by exceptionally strong atmospheric forcing associated with a high North Atlantic

Oscillation index, which drove unusually strong surface cooling and deep winter convection as compared with the previous 12 years, pre-conditioning the region for similarly deep mixing in the winter of 2015/2016 (de Jong and de Steur, 2016; de Jong et al., 2018, in this issue). The spring bloom is evident in elevated surface chlorophyll *a* concentrations from April to early June in both 2015 and 2016 (Figures 2a and 3b).

Observed mixed layer dissolved oxygen concentrations can be interpreted by comparison with oxygen concentrations expected if the surface ocean were in equilibrium with the atmosphere (equilibrium O_2 in Figure 3c). Throughout the winter months, surface oxygen concentrations remain below saturation, indicating ventilation of oxygen-undersaturated deeper waters with a net respiration signature. Oxygen undersaturation persists until the beginning of the spring bloom, when surface oxygen rapidly increases in tandem with the increase in chlorophyll *a*. Once oxygen concentrations reach supersaturation in late April 2015, they remain supersaturated through early October. This, as well as chlorophyll *a* concentrations elevated above baseline values (Figure 3b), suggests that productive conditions of surface net autotrophy extend throughout this period.

Although oxygen measurements are not sufficiently accurate to estimate the total net community production (NCP) in the surface mixed layer, the rapid increase in dissolved oxygen during the 2015 spring bloom from a baseline value of 305 ±2 μmol kg^{-1} during April 1–10 to a maximum value of 402 μmol kg^{-1} on May 11 reflects an increase in the mixed layer oxygen inventory of ~3.0 mol m^{-2} integrated through the ~30 m mixed layer at the time of the oxygen maximum. This increase in oxygen inventory places a lower bound (neglecting oxygen flux to the atmosphere) on the mixed layer NCP during this initial bloom period equivalent to net production of ~2.1 mol C m^{-2}, or 70 mmol C m^{-2} d^{-1} (based on a O_2:C ratio of 1.4; Laws, 1991). Previous estimates of oxygen flux to the atmosphere during the subpolar North Atlantic spring bloom are of comparable magnitude (Quay et al., 2012, and references therein), suggesting that the total NCP during the bloom is likely considerably greater than our lower bound estimate.

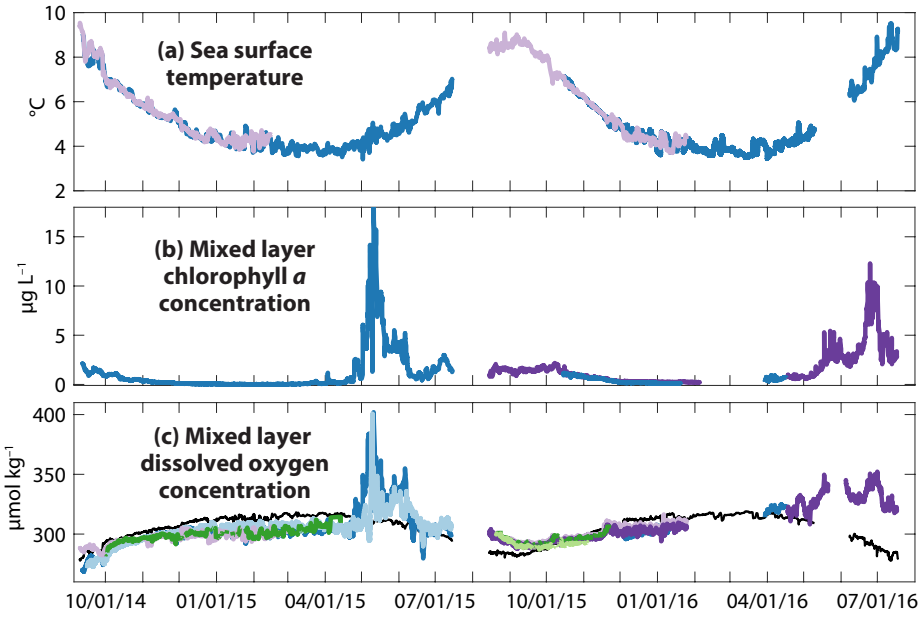

FIGURE 3. Surface mixed layer (a) sea surface temperature, (b) chlorophyll *a* concentration, and (c) dissolved oxygen from the OOI Irminger Sea Array over the first two years of deployment. Data are compiled from multiple array assets (see Figure 2b) to provide nearly continuous data. The oxygen concentration expected if the mixed layer were in equilibrium with the atmosphere, calculated from sea surface temperature and salinity following the equation of Garcia and Gordon (1992), is provided in (c) for comparison with observed concentrations.

SEASONAL CYCLE OF THERMOCLINE RESPIRATION AND WINTER VENTILATION

Observations below the mixed layer allow us to see the seasonal evolution of respiration and ventilation within the seasonal thermocline. Profiler mooring temperature data (Figure 4a) were compared with sea surface temperature (Figure 3a) to determine the base of the mixed layer (Δ0.2°C from the sea surface temperature; de Boyer Montégut et al., 2004). During the stratified spring and summer season, the profiler mooring's surface-most measurements are well below the mixed layer (i.e., the uppermost temperature measurements from the profiler mooring are more than 0.2°C cooler than the sea surface). As the mixed layer deepens in fall and winter, the surface mixed layer penetrates into the seasonal thermocline and ventilates waters that were isolated from contact with the atmosphere during the stratified season. In both 2014 and 2015, mixed layers first reached to 200 m depth in mid-November, with ventilation extending deeper into the water column and progressively eroding seasonal stratification through the winter (red lines in Figure 4).

The dates of initial winter ventilation (the time that the mixed layer first penetrates to a given depth within the thermocline) correspond with a rapid increase in dissolved oxygen concentration at depth as the oxygen-undersaturated thermocline waters are exposed to the atmosphere (Figure 4b,c). Once ventilation has penetrated to a given depth, oxygen concentrations at that depth continue to increase throughout the period of winter convection until stratification is reestablished in spring (Figure 5). Because the

depth of active mixing often decreases in spring prior to stratification of the mixed layer defined based on physical properties, the date of re-stratification in spring is defined based on the maximum oxygen concentration at a given depth (yellow dots in Figure 5, shown for all depths as the yellow lines in Figure 4).

Respiration in the seasonal thermocline is evident in the oxygen decrease over the stratified season (Figure 5). These layers are isolated from contact with the atmosphere, and the seasonal-scale influence of advection is low because the profiler mooring is located near the center of the gyre where the mean currents are relatively weak (de Jong et al., 2018, in this issue). Thus, oxygen decline over the stratified season reflects respiration of organic matter by heterotrophic organisms. We calculate the respiration over the stratified season at each depth interval as the oxygen decrease from the oxygen maximum at the onset of re-stratification (yellow dots in Figure 5) to the oxygen minimum at the end of the stratified season (cyan dots in Figure 5), yielding total respiration rates for all depths from 200–1,000 m within the seasonal thermocline (Figure 6).

Consistent with previous oxygen-based estimates of subsurface respiration (Martz et al., 2008; Hennon et al., 2016) and with canonical expectations for attenuation of organic matter flux with depth (J.M. Martin et al., 1987), total seasonal respiration is greatest near the top of the thermocline and decreases with depth (Figure 6). The duration of the stratified season over which this respiration occurs increases with depth, as re-stratification begins earlier and winter ventilation begins later deeper in the water column (stratification duration ranges from 194 ±1 days at depths from 200–300 m to 280 ±3 days at depths from 750–1,000 m; Figures 4 and 5). The total respiration within each depth interval is stoichiometrically related to an increase in dissolved inorganic carbon due to organic matter remineralization over the course of the stratified season, which is then ventilated back to the atmosphere during winter. Integrated through the 200–1,000 m layer within the seasonal thermocline, ~5.9 mol C m^{-2} was remineralized (8.3 mol O_2 m^{-2} consumed by respiration) over the 2015 stratified season prior to being entrained back into the mixed layer during winter ventilation in 2015/2016. This magnitude of winter ventilation is greater than that previously observed in other deep mixing regions (2.6 mol C m^{-2} in the eastern North Atlantic and 3.6 mol C m^{-2} in the western North Pacific; Körtzinger et al., 2008; Palevsky et al., 2016a), consistent with the Irminger Sea's stronger spring bloom and deeper winter mixing that enhance the importance of thermocline remineralization and winter ventilation.

CONCLUSIONS

Carbon sequestration via the biological pump can be thought of as a "tug of war" between downward flux of organic matter from the surface during the stratified productive season and upward flux of remineralized organic matter during wintertime ventilation. Both of these

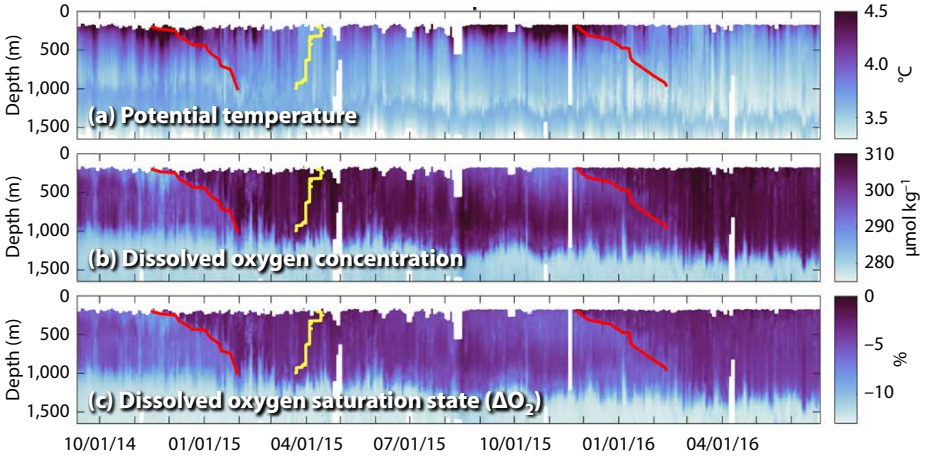

FIGURE 4. Time series of (a) potential temperature, (b) dissolved oxygen concentration, and (c) dissolved oxygen saturation state

$$(\Delta O_2 = \left(\frac{O_{2,\,observed}}{O_{2,\,equilibrium}} - 1\right) * 100)$$

from the profiler mooring. Red lines indicate the beginning of winter ventilation in each year (determined as the time that the mixed layer first penetrates to a given depth), and yellow lines indicate the end of winter ventilation in 2015 (determined as the date of the late winter-early spring oxygen maximum at each depth; see Figure 5).

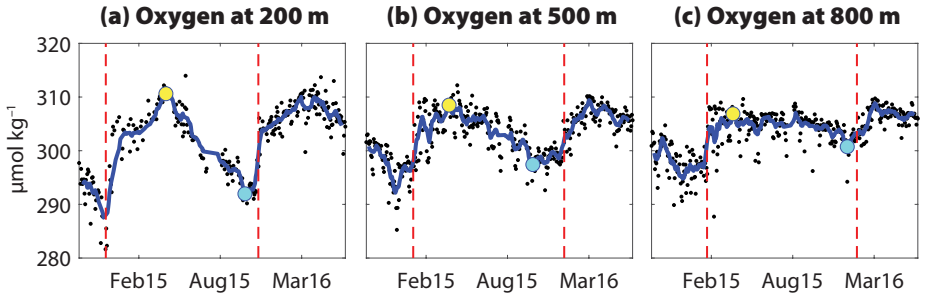

FIGURE 5. Examples of dissolved oxygen time series at (a) 200 m, (b) 500 m, and (c) 800 m depth from the profiler mooring over the first two years' deployment of the OOI Irminger Sea Array. Blue lines show the smoothed time series, determined as a 10-point filtered mean of all dissolved oxygen values gridded to each depth (black points). Red dashed lines indicate the date of initial winter ventilation in each year, determined as the time that the mixed layer first penetrates to the given depth. The end of winter ventilation (cyan dots) in spring 2015 is determined as the maximum dissolved oxygen concentration. The oxygen decrease from the end of winter ventilation (yellow dots) to the minimum oxygen concentration at the end of the stratified season (cyan dots) shows respiration of organic carbon within the seasonal thermocline.

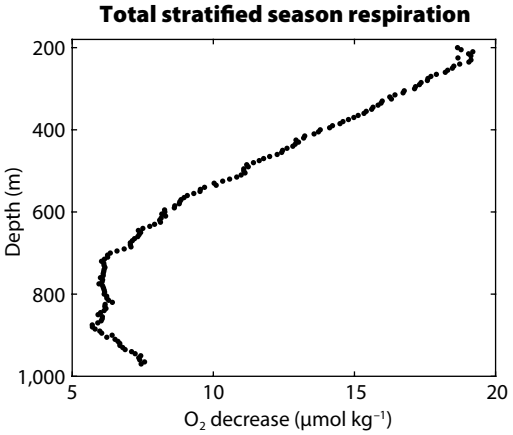

FIGURE 6. Total respiration in the seasonal thermocline (200–1,000 m depth) over the 2015 stratified season, calculated as the oxygen decrease from the end of winter ventilation in spring 2015 to the oxygen minimum at the end of the stratified season (from the yellow to the cyan dots in Figure 5). Thermocline respiration integrated through this full layer is 8.3 mol O_2 m^{-2}, representing 5.9 mol C m^{-2} ventilated back to the atmosphere the subsequent winter (O_2:C ratio of 1.4; Laws, 1991).

players "tug" especially hard in the subpolar North Atlantic (Figure 1). Data from the first two years of the new OOI Irminger Sea Array provide the first simultaneous observations of the seasonal progression of the biological pump in both the surface mixed layer and the seasonal thermocline in the subpolar North Atlantic Ocean. The spring bloom during April–May each year was associated with a dramatic increase in mixed layer dissolved oxygen, reflecting significant net autotrophic production during this period (Figures 2 and 3). Below the mixed layer, oxygen decline over the 2015 stratified season indicated high remineralization rates within the seasonal thermocline totaling ~5.9 mol C m^{-2} between 200 m and 1,000 m—greater than the total annual export from the surface in most parts of the ocean (Figures 5 and 6; Emerson, 2014). Deep winter convection extending below 1,000 m ventilated this respiration signature from the seasonal thermocline, maintaining surface dissolved oxygen concentrations below saturation throughout the winter months despite vigorous gas exchange acting to return mixed layer oxygen to saturation (Figures 3c and 4).

These results highlight the importance of accounting for remineralization within the seasonal thermocline and ventilation of respired carbon back to the atmosphere during winter mixing in order to accurately determine the influence of the biological pump on carbon sequestration, particularly in deep convection regions such as the Irminger Sea. However, a limitation of this analysis is that mixed layer oxygen measurements cannot be calibrated with sufficient accuracy to enable a mass balance calculation of annual net community production at the winter ventilation depth or export from the mixed layer over the stratified season. The accuracy and utility of oxygen measurements from the Irminger Sea and other OOI arrays could be improved by configuring the glider oxygen sensors for in situ air calibration when surfacing between profiles (Nicholson and Feen, 2017), an approach previously proven on long-term Argo float deployments (Johnson et al., 2015; Bushinsky et al., 2016).

Given that winter convection over the initial two years of the OOI Irminger Sea Array's deployment was significantly deeper than the climatological mean over the previous decade (de Jong and de Steur, 2016), future observations will play an important role in contextualizing the initial look into the Irminger Sea biological pump presented here. Ongoing time-series observations at the OOI Array, ideally with improved calibration of biogeochemical sensors, will enable future analysis of interannual variability in the timing and magnitude of the spring bloom, spring and summer net autotrophy in the surface mixed layer, thermocline remineralization, and winter ventilation. Biogeochemical sensor data from the OOI global arrays and other year-round observing systems (e.g., Biogeochemical Argo floats; Johnson and Claustre, 2016) provide a powerful tool for investigating carbon cycling throughout the full annual cycle in the previously undersampled high-latitude ocean.

SUPPLEMENTARY MATERIALS

Supplementary Text, Figures S1 and S2, and Tables S1 and S2, include details on all data used in this analysis and are available online at https://doi.org/10.5670/oceanog.2018.108.

REFERENCES

Antia, N., R. Peinert, D. Hebbeln, U. Bathmann, U. Fehner, and B. Zeitzschel. 2001. Basin-wide particulate carbon flux in the Atlantic Ocean: Regional export patterns and potential for atmospheric CO_2 sequestration. *Global Biogeochemical Cycles* 15(4):845–862, https://doi.org/10.1029/2000gb001376.

Behrenfeld, M.J., and E.S. Boss. 2014. Resurrecting the ecological underpinnings of ocean plankton blooms. *Annual Review of Marine Science* 6(1):167–194, https://doi.org/10.1146/annurev-marine-052913-021325.

Bittig, H.C., and A. Körtzinger. 2015. Tackling oxygen optode drift: Near-surface and in-air oxygen optode measurements on a float provide an accurate in situ reference. *Journal of Atmospheric and Oceanic Technology* 32(8):1,536–1,543, https://doi.org/10.1175/JTECH-D-14-00162.1.

Bittig, H.C., and A. Körtzinger. 2017. Technical note: Update on response times, in-air measurements, and in situ drift for oxygen optodes on profiling platforms. *Ocean Science* 13(1):1–11, https://doi.org/10.5194/os-13-1-2017.

Briggs, N., M.J. Perry, I. Cetinić, C. Lee, E. D'Asaro, A.M. Gray, and E. Rehm. 2011. High-resolution observations of aggregate flux during a sub-polar North Atlantic spring bloom. *Deep Sea Research Part I* 58(10):1,031–1,039, https://doi.org/10.1016/j.dsr.2011.07.007.

Buesseler, K.O., P. Michael, H.D. Livingston, and K. Cochrant. 1992. Carbon and nitrogen export during the JGOFS North Atlantic Bloom Experiment estimated from ^{234}Th:^{238}U disequilibria. *Deep Sea Research* 39(7–8):1,115–1,137, https://doi.org/10.1016/0198-0149(92)90060-7.

Bushinsky, S.M., S.R. Emerson, S.C. Riser, and D.D. Swift. 2016. Accurate oxygen measurements on modified Argo floats using in situ air calibrations. *Limnology and Oceanography: Methods* 14:491–505, https://doi.org/10.1002/lom3.10107.

Church, M.J., M.W. Lomas, and F. Muller-Karger. 2013. Sea change: Charting the course for biogeochemical ocean time-series research in a new millennium. *Deep Sea Research Part II* 93:2–15, https://doi.org/10.1016/j.dsr2.2013.01.035.

Ciais, P., C. Sabine, G. Bala, L. Bopp, V. Brovkin, J. Canadell, A. Chhabra, R. DeFries, J. Galloway, M. Heimann, and others. 2013. Carbon and other biogeochemical cycles. Pp. 465–570. In *Climate Change 2013 - The Physical Science Basis. Contribution of Working Group I to the Fifth Assessment Report of the Intergovernmental Panel on Climate Change*. T.F. Stocker, D. Qin, G.-K. Plattner, M. Tignor, S.K. Allen, J. Boschung, A. Nauels, Y. Xia, and V. Bex, eds, Cambridge University Press, Cambridge, United Kingdom and New York, NY, USA, https://doi.org/10.1017/CBO9781107415324.015.

D'Asaro, E.A., and C. McNeil. 2013. Calibration and stability of oxygen sensors on autonomous floats. *Journal of Atmospheric and Oceanic Technology* 30:1,896–1,906, https://doi.org/10.1175/JTECH-D-12-00222.1.

Dall'Olmo, G., J. Dingle, L. Polimene, R.J.W. Brewin, and H. Claustre. 2016. Substantial energy input to the mesopelagic ecosystem from the seasonal mixed-layer pump. *Nature Geoscience* 9:820–823, https://doi.org/10.1038/ngeo2818.

de Boyer Montégut, C., G. Madec, A.S. Fischer, A. Lazar, and D. Iudicone. 2004. Mixed layer depth over the global ocean: An examination of profile data and a profile-based climatology. *Journal of Geophysical Research* 109, C12003, https://doi.org/10.1029/2004JC002378.

de Jong, M.F., and L. de Steur. 2016. Strong winter cooling over the Irminger Sea in winter 2014–2015, exceptional deep convection, and the emergence of anomalously low SST. *Geophysical Research Letters* 43(13):7,106–7,113, https://doi.org/10.1002/2016GL069596.

de Jong, M.F., M. Oltmanns, J. Karstensen, and L. de Steur. 2018. Deep convection in the Irminger Sea observed with a dense mooring array. *Oceanography* 31(1):50–59, https://doi.org/10.5670/oceanog.2018.109.

de Jong, M.F., H.M. Van Aken, K. Våge, and R.S. Pickart. 2012. Convective mixing in the central Irminger Sea: 2002–2010. *Deep Sea Research Part I* 63:36–51, https://doi.org/10.1016/j.dsr.2012.01.003.

DeVries, T., F. Primeau, and C. Deutsch. 2012. The sequestration efficiency of the biological pump. *Geophysical Research Letters* 39, L13601, https://doi.org/10.1029/2012GL051963.

Emerson, S. 2014. Annual net community production and the biological carbon flux in the ocean. *Global Biogeochemical Cycles* 28:14–28, https://doi.org/10.1002/2013GB004680.

Emerson, S., and S. Bushinsky. 2014. Oxygen concentrations and biological fluxes in the open ocean. *Oceanography* 27(1):168–171, https://doi.org/10.5670/oceanog.2014.20.

Field, C.B., M.J. Behrenfeld, J.T. Randerson, and P. Falkowski. 1998. Primary production of the biosphere: Integrating terrestrial and oceanic components. *Science* 281(5374):237–240, https://doi.org/10.1126/science.281.5374.237.

Garcia, H.E., and L.I. Gordon. 1992. Oxygen solubility in seawater: Better fitting solubility equations. *Limnology and Oceanography* 37(6):1,307–1,312, https://doi.org/10.4319/lo.1992.37.6.1307.

Hennon, T.D., S.C. Riser, and S. Mecking. 2016. Profiling float-based observations of net respiration beneath the mixed layer. *Global Biogeochemical Cycles* 30:920–932, https://doi.org/10.1002/2016GB005380.

Henson, S.A., C. Beaulieu, and R. Lampitt. 2016. Observing climate change trends in ocean biogeochemistry: When and where. *Global Change Biology* 22:1,561–1,571, https://doi.org/10.1111/gcb.13152.

Henson, S.A., J.P. Dunne, and J.L. Sarmiento. 2009. Decadal variability in North Atlantic phytoplankton blooms. *Journal of Geophysical Research* 114(4):1–11, https://doi.org/10.1029/2008JC005139.

Henson, S.A., I. Robinson, J.T. Allen, and J.J. Waniek. 2006. Effect of meteorological conditions on interannual variability in timing and magnitude of the spring bloom in the Irminger Basin, North Atlantic. *Deep Sea Research Part I* 53:1,601–1,615, https://doi.org/10.1016/j.dsr.2006.07.009.

Johnson, K.S., and H. Claustre. 2016. Bringing Biogeochemistry into the Argo Age. *Eos* 97, https://doi.org/10.1029/2016EO062427.

Johnson, K.S., J.N. Plant, S.C. Riser, and D. Gilbert. 2015. Air oxygen calibration of oxygen optodes on a profiling float array. *Journal of Atmospheric and Oceanic Technology* 32(11):2,160–2,172, https://doi.org/10.1175/JTECH-D-15-0101.1.

Khatiwala, S., F. Primeau, and T. Hall. 2009. Reconstruction of the history of anthropogenic CO_2 concentrations in the ocean. *Nature* 462(7271):346–349, https://doi.org/10.1038/nature08526.

Körtzinger, A., U. Send, R.S. Lampitt, S. Hartman, D.W.R. Wallace, J. Karstensen, M.G. Villagarcia, O. Llinás, and M.D. DeGrandpre. 2008. The seasonal pCO_2 cycle at 49°N/16.5°W in the northeastern Atlantic Ocean and what it tells us about biological productivity. *Journal of Geophysical Research* 113, C04020, https://doi.org/10.1029/2007JC004347.

Laws, E.A. 1991. Photosynthetic quotients, new production and net community production in the open ocean. *Deep Sea Research* 38(1):143–167, https://doi.org/10.1016/0198-0149(91)90059-O.

Laws, E.A., E. D'Sa, and P. Naik. 2011. Simple equations to estimate ratios of new or export production to total production from satellite-derived estimates of sea surface temperature and primary production. *Limnology and Oceanography: Methods* 9:593–601, https://doi.org/10.4319/lom.2011.9.593.

Le Quéré, C., R.M. Andrew, J.G. Canadell, S. Sitch, J.I. Korsbakken, G.P. Peters, A.C. Manning, T.A. Boden, P.P. Tans, R.A. Houghton, and others. 2016. Global carbon budget 2016. *Earth System Science Data* 8:605–649, https://doi.org/10.5194/essd-8-605-2016.

Martin, J.M., G.A. Knauer, D.M. Karl, and W.W. Broenkow. 1987. VERTEX: Carbon cycling in the Northeast Pacific. *Deep Sea Research* 34(2):267–285, https://doi.org/10.1016/0198-0149(87)90086-0.

Martin, P., R.S. Lampitt, M.J. Perry, R. Sanders, C. Lee, and E. D'Asaro. 2011. Export and mesopelagic particle flux during a North Atlantic spring diatom bloom. *Deep Sea Research Part I* 58:338–349, https://doi.org/10.1016/j.dsr.2011.01.006.

Martz, T.R., K.S. Johnson, and S.C. Riser. 2008. Ocean metabolism observed with oxygen sensors on profiling floats in the South Pacific. *Limnology and Oceanography* 53(5, part 2):2,094–2,111, https://doi.org/10.4319/lo.2008.53.5_part_2.2094.

Nicholson, D.P., and M.L. Feen. 2017. Air calibration of an oxygen optode on an underwater glider. *Limnology and Oceanography: Methods* 15:495–502, https://doi.org/10.1002/lom3.10177.

Oschlies, A., and P. Kahler. 2004. Biotic contribution to air-sea fluxes of CO_2 and O_2 and its relation to new production, export production, and net community production. *Global Biogeochemical Cycles* 18, GB1015, https://doi.org/10.1029/2003GB002094.

Palevsky, H.I., P.D. Quay, D.E. Lockwood, and D.P. Nicholson. 2016a. The annual cycle of gross primary production, net community production, and export efficiency across the North Pacific Ocean. *Global Biogeochemical Cycles* 30:361–380, https://doi.org/10.1002/2015GB005318.

Palevsky, H.I., P.D. Quay, and D.P. Nicholson. 2016b. Discrepant estimates of primary and export production from satellite algorithms, a biogeochemical model and geochemical tracer measurements in the North Pacific Ocean. *Geophysical Research Letters* 43:8,645–8,653, https://doi.org/10.1002/2016GL070226.

Pickart, R.S., M.A. Spall, M.H. Ribergaard, G.W.K. Moore, and R.F. Milliff. 2003. Deep convection in the Irminger Sea forced by the Greenland tip jet. *Nature* 424(6945):152–156, https://doi.org/10.1038/nature01729.

Quay, P., J. Stutsman, and T. Steinhoff. 2012. Primary production and carbon export rates across the subpolar N. Atlantic Ocean basin based on triple oxygen isotope and dissolved O_2 and Ar gas measurements. *Global Biogeochemical Cycles* 26, GB2003, https://doi.org/10.1029/2010GB004003.

Sabine, C.L., R.A. Feely, N. Gruber, R.M. Key, K. Lee, J.L. Bullister, R. Wanninkhof, C. Wong, D.W.R. Wallace, B. Tilbrook, and others. 2004. The oceanic sink for anthropogenic CO_2. *Science* 305:367–371, https://doi.org/10.1126/science.1097403.

Sabine, C.L., and T. Tanhua. 2010. Estimation of anthropogenic CO_2 inventories in the ocean. *Annual Review of Marine Science* 2:175–198, https://doi.org/10.1146/annurev-marine-120308-080947.

Sanders, R., S.A. Henson, M. Koski, C.L. De La Rocha, S.C. Painter, A.J. Poulton, J. Riley, B. Salihoglu, A. Visser, A. Yool, and others. 2014. The biological carbon pump in the North Atlantic. *Progress in Oceanography* 129:200–218, https://doi.org/10.1016/j.pocean.2014.05.005.

Sarmiento, J.L., and N. Gruber. 2006. *Ocean Biogeochemical Dynamics*. Princeton University Press, Princeton, NJ, 526 pp.

Siegel, D.A., K.O. Buesseler, S.C. Doney, S.F. Sailley, M.J. Behrenfeld, and P.W. Boyd. 2014. Global assessment of ocean carbon export by combining satellite observations and food-web models. *Global Biogeochemical Cycles* 28:181–196, https://doi.org/10.1002/2013GB004743.

Stukel, M.R., M. Kahru, C.R. Benitez-Nelson, M. Decima, R. Goericke, M.R. Landry, and M.D. Ohman. 2015. Using Lagrangian-based process studies to test satellite algorithms of vertical carbon flux in the eastern North Pacific Ocean. *Journal of Geophysical Research* 120:7,208–7,222, https://doi.org/10.1002/2015JC011264.

Takeshita, Y., T.R. Martz, K.S. Johnson, J.N. Plant, D. Gilbert, S.C. Riser, C. Neill, and B. Tilbrook. 2013. A climatology-based quality control procedure for profiling float oxygen data. *Journal of Geophysical Research* 118:5,640–5,650, https://doi.org/10.1002/jgrc.20399.

Volk, T., and M.I. Hoffert. 1985. Ocean carbon pumps: Analysis of relative strengths and efficiencies in ocean-driven atmospheric CO_2 changes. Pp. 99–110 in *The Carbon Cycle and Atmospheric CO_2 Natural Variations Archean to Present*. E.T. Sundquist and W.S. Broecker, eds, Geophysical Monograph Series, vol. 32, American Geophysical Union, Washington, DC.

ACKNOWLEDGMENTS

We are grateful to the many people involved in the planning, deployment, operation, and data management of the Ocean Observatories Initiative, and to the National Science Foundation for OOI funding. We thank Robert Weller, Paul Quay, Robert Vaillancourt, and an anonymous reviewer for constructive feedback that improved the manuscript. Hilary Palevsky acknowledges support from the Postdoctoral Scholar Program at the Woods Hole Oceanographic Institution, with funding provided by the Weston Howland Jr. Postdoctoral Scholarship.

AUTHORS

Hilary I. Palevsky (hpalevsky@whoi.edu) is Postdoctoral Scholar and **David P. Nicholson** is Associate Scientist, both in the Department of Marine Chemistry and Geochemistry, Woods Hole Oceanographic Institution, Woods Hole, MA, USA.

ARTICLE CITATION

Palevsky, H.I., and D.P. Nicholson. 2018. The North Atlantic biological pump: Insights from the Ocean Observatories Initiative Irminger Sea Array. *Oceanography* 31(1):42–49, https://doi.org/10.5670/oceanog.2018.108.